THE FLOW, TEMPERATURE AND CONCENTRATION FIELDS IN A RADIO-FREQUENCY ARGON-HELIUM PLASMA

TAKAYUKI WATANABE, KAZUHIKO YANASE, TAKUYA HONDA AND ATUSHI KANZAWA

Department of Chemical Engineering, Tokyo Institute of Technology, Tokyo 152

Key Words: High Temperature, Plasma Chemistry, Numerical Simulation, Thermal Plasma, RF Plasma, Modeling, Water-Cooled Probe

The numerical simulation of an RF argon-helium thermal plasma under atmospheric pressure was performed. The two-dimensional continuity, momentum, energy and species equations along with the electromagnetic equations were solved simultaneously with the SIMPLER algorithm. The physical properties of the argon-helium mixed plasma were taken into account. The plasma velocity, temperature and concentration were measured with a water-cooled probe. The numerical results were in good agreement with the experimental ones. The results demonstrate the existence of an inward radial flow induced by the electromagnetic pumping effect. The recirculating eddy formed by the inward radial flow becomes stronger in an argon-helium plasma than that in an argon plasma. A uniform distribution of helium concentration is obtained upstream from the discharge region.

Introduction

A radio-frequency (RF) inductively coupled plasma offers a clean high-energy source. The main advantage of the RF plasma is that reactive gases can be used as well as inert gases. The RF plasma has been used for chemical synthesis, plasma spraying and extractive metallurgy, and more extensively in recent years for producing ultrafine powders of various materials.

The temperature and flow fields in an RF plasma have been studied in order to increase the efficiency of chemical reactions and to enlarge the equipment to industrial scale. Measurements of these fields in an RF plasma are rather complex and difficult to obtain. The fields are disturbed by the measurement probe. Numerical simulation of these fields has thus been required. In the early stage of numerical simulation, the temperature field is calculated with a one-dimensional model.[10] Boulos[1] calculated the two-dimensional flow and temperature fields and the one-dimensional electromagnetic field, employing the vorticity-stream function. Recently, Mostaghimi *et al.*[12] adopted the SIMPLER algorithm,[13] which greatly increased the stability and convergence rate for the solution of the continuity, momentum and energy equations.

The numerical simulation of a mixed gas in an RF plasma is required in connection with the investigation of reactions in the plasma. A few authors have considered theoretical models of a mixed gas in an RF plasma. Guo-Ying and Ching-Wen[7] presented a model of the RF plasma with argon and reactant gases. However, the chemical reactions and physical properties of the mixed gas other than the density and specific heat were not taken into account in their model.

In the present work, the physical properties of a mixed gas were taken into account. The RF argon-helium thermal plasma under atmospheric pressure has been formulated to investigate the behavior of the mixed gas in the plasma. The two-dimensional continuity, momentum, energy and species equations along with the one-dimensional electromagnetic equations were solved simultaneously.

The plasma velocity, temperature and concentrations were measured with a water-cooled probe. Numerical and experimental results were compared.

1. Numerical Simulation

1.1 Basic model and assumptions

The fields of flow, temperature and concentration in an RF plasma torch were calculated by solving the two-dimensional continuity, momentum, energy and species equations along with the one-dimensional electromagnetic equations. The RF plasma torch configuration used in this numerical simulation is shown in **Fig. 1**. Gases issue from circular slits of 2 mm width. Argon issues both from the inner slit (flow rate: $Q1$) and the outer slit ($Q2$), and helium from the outer slit ($Q3$). The model dimensions are the same as for the experimental apparatus described later.

* Received August 24, 1989. Correspondence concerning this article should be addressed to T. Watanabe. K. Yanase is now with Kirin Brewery Co., Ltd., Kyoto 601.

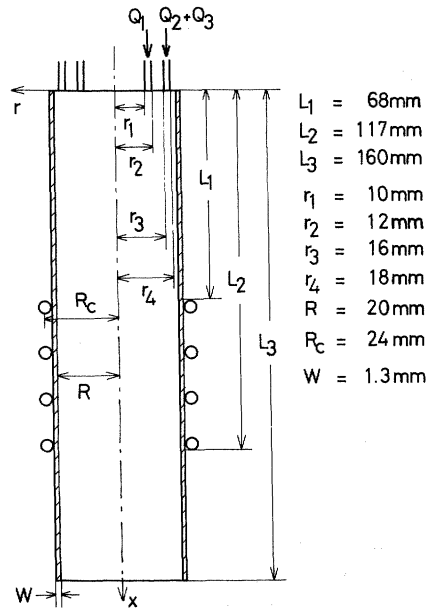

Fig. 1. Schematic of inductively coupled plasma torch model

The following assumptions were made for the present model:

a) Steady-state laminar flow
b) Local thermodynamic equilibrium
c) Axial symmetry
d) Optically thin plasma
e) Negligible viscous dissipation
f) Negligible displacement current

1.2 Governing equations and boundary conditions

The governing equations in cylindrical coordinates are formulated as follows:

Continuity:

$$\frac{1}{r}\cdot\frac{\partial}{\partial r}(r\rho v)+\frac{\partial}{\partial x}(\rho u)=0 \tag{1}$$

Momentum:

$$\rho\left(u\frac{\partial u}{\partial x}+v\frac{\partial u}{\partial r}\right)=-\frac{\partial p}{\partial x}+2\frac{\partial}{\partial x}\left(\mu\frac{\partial u}{\partial x}\right)+\frac{1}{r}\cdot\frac{\partial}{\partial r}\left[\mu r\left(\frac{\partial u}{\partial r}+\frac{\partial v}{\partial x}\right)\right] \tag{2}$$

$$\rho\left(u\frac{\partial v}{\partial x}+v\frac{\partial v}{\partial r}\right)=-\frac{\partial p}{\partial r}+\frac{2}{r}\cdot\frac{\partial}{\partial r}\left(\mu r\frac{\partial v}{\partial r}\right)+\frac{\partial}{\partial x}\left[\mu\left(\frac{\partial u}{\partial r}+\frac{\partial v}{\partial x}\right)\right]-\frac{2\mu v}{r^2}+F_r \tag{3}$$

Energy:

$$\rho\left(u\frac{\partial h}{\partial x}+v\frac{\partial h}{\partial r}\right)=\frac{1}{r}\cdot\frac{\partial}{\partial r}\left(r\frac{k}{C_p}\cdot\frac{\partial h}{\partial r}\right)+\frac{\partial}{\partial x}\left(\frac{k}{C_p}\cdot\frac{\partial h}{\partial x}\right)+P-Q_r \tag{4}$$

The volumetric radiation loss, Q_r, was calculated from the equations proposed by Miller and Ayen[11] based on the data by Evans and Tankin.[5]

Species:

$$\rho\left(u\frac{\partial C_{w_i}}{\partial x}+v\frac{\partial C_{w_i}}{\partial r}\right)=\frac{1}{r}\cdot\frac{\partial}{\partial r}\left(\rho D_i r\frac{\partial C_{w_i}}{\partial r}\right)+\frac{\partial}{\partial x}\left(\rho D_i\frac{\partial C_{w_i}}{\partial x}\right) \tag{5}$$

The corresponding one-dimensional (r-direction) electromagnetic equations are as follows:

$$\frac{dE_\theta}{dr}=-\frac{E_\theta}{r}-\xi\omega H_x\sin\chi \tag{6}$$

$$\frac{dH_x}{dr}=-\sigma E_\theta\cos\chi \tag{7}$$

$$\frac{\partial\chi}{dr}=\frac{\sigma E_\theta}{H_x}\sin\chi-\frac{\xi\omega H_x}{E_\theta}\cos\chi \tag{8}$$

These can be used to calculate the local power dissipation P and the radial body force F_r as follows:

$$P=\sigma {E_\theta}^2 \tag{9}$$

$$F_r=\xi\sigma E_\theta H_x\cos\chi \tag{10}$$

The governing Eqs. (1)–(5) require boundary conditions as follows:

Inlet ($x=0$):

$$u=\begin{cases} Q1/\pi(r_2^2-r_1^2), & r_1<r<r_2 \\ (Q2+Q3)/\pi(r_4^2-r_3^2), & r_3<r<r_4 \\ 0, & \text{the other positions}\end{cases} \tag{11}$$

$$v=0 \tag{12}$$

$$C_{w_{He}}=\frac{Q3\cdot m_{He}}{(Q1+Q2)m_{Ar}+Q3\cdot m_{He,}}\quad r_3<r<r_4 \tag{13}$$

$$T=300\ \mathrm{K} \tag{14}$$

Centerline ($r=0$):

$$\frac{\partial u}{\partial r}=\frac{\partial h}{\partial r}=\frac{\partial C_{w_{He}}}{\partial r}=v=0 \tag{15}$$

Wall ($r=R$):

$$u=v=\frac{\partial C_{w_{He}}}{\partial r}=0 \tag{16}$$

$$\frac{k}{C_P}\cdot\frac{\partial h}{\partial r}=\frac{k_c}{W}\cdot(T-T_{W_0}),\quad (T_{W_0}=300\ \mathrm{K}) \tag{17}$$

Exit ($x=L$):

$$\frac{\partial u}{\partial x}=\frac{\partial v}{\partial x}=\frac{\partial h}{\partial x}=\frac{\partial C_{w_{He}}}{\partial x}=0 \tag{18}$$

The boundary conditions for the electromagnetic fields Eqs. (6)–(8) are set at the centerline of the torch

as follows:

$$\chi=\frac{\pi}{2}, \qquad \frac{d\chi}{dr}=0 \tag{19}$$

$$E_\theta=0, \qquad \frac{dE_\theta}{dr}=-\frac{\xi\omega H_x}{2} \tag{20}$$

$$H_x=H_c(x), \quad \frac{dH_x}{dr}=0 \tag{21}$$

where

$$H_c(x)=\frac{NI}{2(L_2-L_1)}\left[\frac{L_2-x}{(R_c^2+(L_2-x)^2)^{0.5}}-\frac{L_1-x}{(R_c^2+(L_1-x)^2)^{0.5}}\right]$$

1.3 Thermodynamic and transport properties

The physical properties of an argon-helium mixed plasma were obtained from the following relationships.

The thermal conductivity and viscosity of argon were taken from the data by Devoto[3] and those of helium from Devoto and Li.[4] The thermal conductivity of an argon-helium mixed gas was estimated using the Wassiljewa equation,[14] while the Surtherland equation[14] was employed to estimate the viscosity of the mixture.

The diffusion coefficient was evaluated from the equation by Hirschfelder *et al.*[8]

The specific heat at constant pressure of an argon-helium plasma can be written using a mass fraction:

$$C_{P_{\text{mix}}}=C_{w_{\text{Ar}}}\cdot C_{P_{\text{Ar}}}+C_{w_{\text{He}}}\cdot C_{P_{\text{He}}} \tag{22}$$

The specific heat of argon was taken from the data by Hsu and Pfender.[9] The ionization of helium is negligible below 10,000 K. The specific heat of helium was defined as follows:

$$C_{P_{\text{He}}}=\frac{5k_b}{2m_{\text{He}}} \tag{23}$$

The density was calculated using a number density:

$$\rho=m_{\text{Ar}}(n_{\text{Ar}}+n_i)+m_{\text{He}}n_{\text{He}} \tag{24}$$

The number densities were calculated from the Saha equation:

$$\frac{n_i n_e}{n_{\text{Ar}}}=2\frac{(2\pi m_e k_b T)^{3/2}}{h_p^3}\cdot\frac{U_{i+1}}{U_i}\exp\left(-\frac{E_i}{k_b T}\right) \tag{25}$$

The electrical conductivity was assumed to be equal to that of argon[3] owing to the negligible ionization of helium.

1.4 Calculation procedure

The governing Eqs. (1)–(5) were solved using the SIMPLER algorithm.[13] The SIMPLER (Semi-Implicit Method for Pressure-Linked Equation Revised) algorithm is a general algorithm for the solution of elliptic fluid flow, heat transfer and mass transfer. The electromagnetic field Eqs. (6)–(8) were solved using a fourth-order Runge-Kutta method.

The calculations were performed for a 10×16 grid system in the radial and axial directions, respectively. The velocities in radial and axial directions were located on staggered points between the grid points of the temperature, pressure and concentration fields. A convergence criterion was that the mass balance be satisfied to within 0.1%.

1.5 Calculation results

Computations were performed for an argon-helium plasma operated at a power level of 8 kW with different gas flow rates of argon and helium.

1) An argon plasma The calculated streamlines and isotherms for an argon RF plasma are shown in **Figs. 2(a)** and **(b)**, respectively. Argon issues at 25 litre/min ($Q1=10$ litre/min, $Q2=15$ litre/min).

The dimensionless stream lines are based on the total input flow rate. A recirculating eddy is formed because of a strong inward radial flow induced by the electromagnetic pumping in the coil region. The eddy causes a back flow.

The isotherms show that the highest temperature (10,500 K) exists in the coil region and is off-center on account of the strong electric field in the outer region of the torch.

2) An argon-helium plasma The calculated streamlines, isotherms and concentration contours in an argon-helium mixed plasma are shown in **Figs. 3(a)–(c)**. Argon issues at 15 litre/min ($Q1=10$ litre/min, $Q2=5$ litre/min) and helium at 10 litre/min ($Q3$).

The streamlines demonstrate that the recirculating eddy formed by the electromagnetic pumping becomes stronger than that in an argon RF plasma. The strong eddy is induced by strong Lorentz force; the strong Lorentz force is attributed to the reduced density due to helium addition.

The isotherms indicate that the temperature gradient is more gentle near the quartz tube and the hot spot is closer to the centerline of the torch for the argon-helium plasma than for the argon plasma. The higher thermal conductivity due to helium addition leads to a larger heat loss to the quartz tube.

The concentration contours indicate that the diffusion rate of helium is very high. The distribution of helium becomes uniform above the recirculating eddy. The high diffusion rate is brought about by the recirculating eddy.

Figure 4 represents the radial profiles of axial and radial velocities at $x=90$ mm where the recirculating eddy is formed. Thesse profiles are at the same total flow rate but at different helium input concentrations. Higher helium input concentration leads to lower axial velocity and to higher radial velocity. The strong eddy

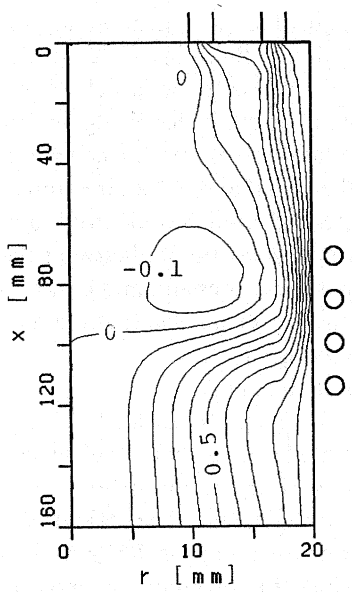

Fig. 2(a). Streamlines (Ar: $Q1 = 10$ litre/min, $Q2 = 15$ litre/min)

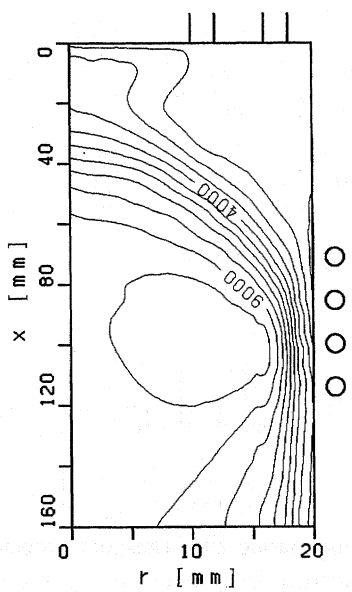

Fig. 2(b). Isotherms (Ar: $Q1 = 10$ litre/min, $Q2 = 15$ litre/min)

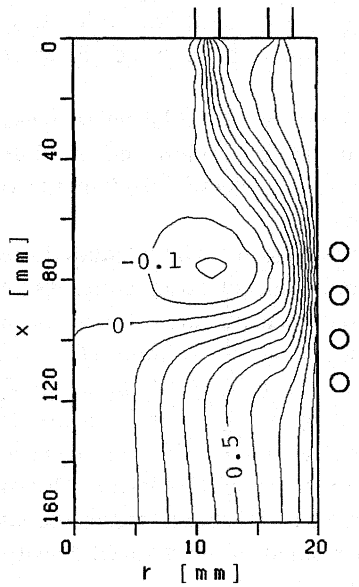

Fig. 3(a). Streamlines (Ar: $Q1 = 10$ litre/min, $Q2 = 5$ litre/min; He: $Q3 = 10$ litre/min)

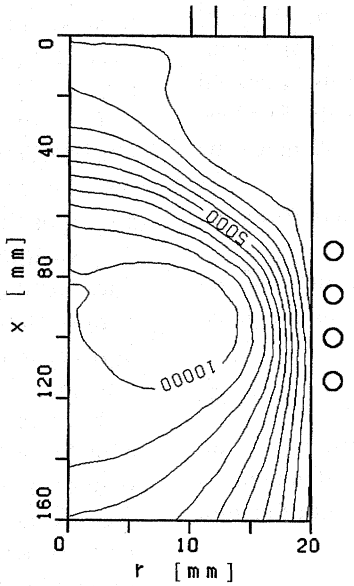

Fig. 3(b). Isotherms (Ar: $Q1 = 10$ litre/min, $Q2 = 5$ litre/min; He: $Q3 = 10$ litre/min)

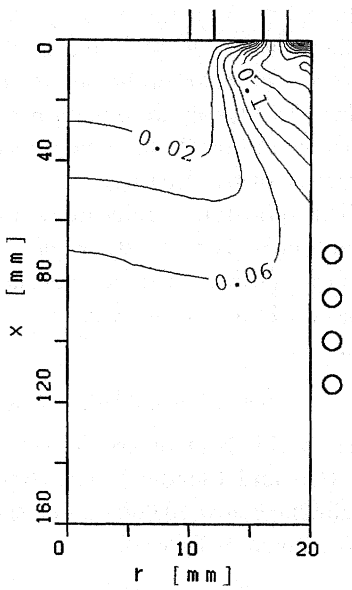

Fig. 3(c). Concentration contours of helium (Ar: $Q1 = 10$ litre/min, $Q2 = 5$ litre/min; He: $Q3 = 10$ litre/min)

is caused by helium addition and it modifies the velocity fields.

The radial temperature profiles are shown in **Fig. 5**. The temperature in the hot spot is almost the same at different helium input concentrations. The temperature near the quartz tube decreases with increasing helium concentration owing to the high thermal conductivity of helium. The maximum approaches the centerline with increasing helium concentration.

Modification of the fields in an RF plasma due to helium addition is useful for plasma processing. The recirculating eddy formed by the electromagnetic pumping effect becomes stronger in an argon-helium plasma than that in an argon plasma. The strong eddy results in uniform distribution of reactants upstream from the high-temperature region.

2. Experimental

2.1 Plasma generator

The plasma generator consisted of a plasma torch and a power supply (4 MHz, 35 kW max.). The plasma torch, shown in **Fig. 6**, consisted of a quartz tube and a working induction coil (4 turns); the coil was positioned between 68 mm and 117 mm below the gas inlet position. The torch was prevented from melting by water cooling.

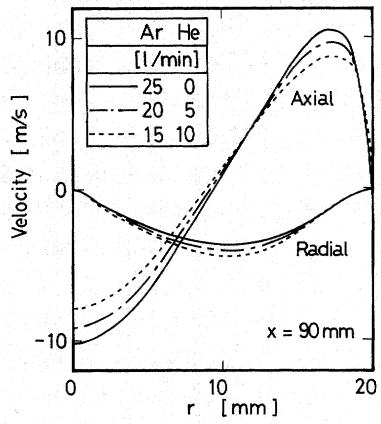

Fig. 4. Radial profiles of axial and radial velocities at $x=90$ mm

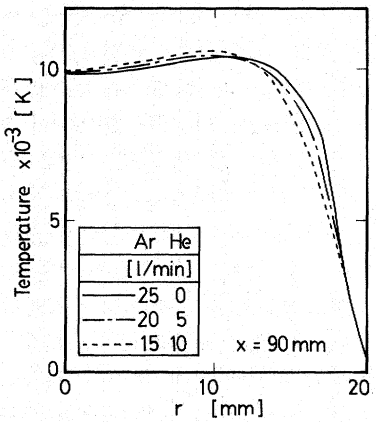

Fig. 5. Radial profiles of temperature at $x=90$ mm

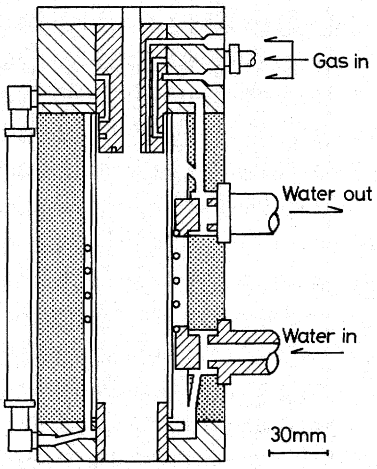

Fig. 6. Schematic of inductively coupled plasma torch

2.2 Measurements

The velocity, temperature and concentrations in the plasma were measured by a water-cooled probe. The probe configuration proposed by Grey *et al.*[6] for plasma measurements is presented in **Fig. 7**. Cooling water entered through the outer coolant channel to the probe tip and returned through the inner coolant channel. The thermocouples were located at the

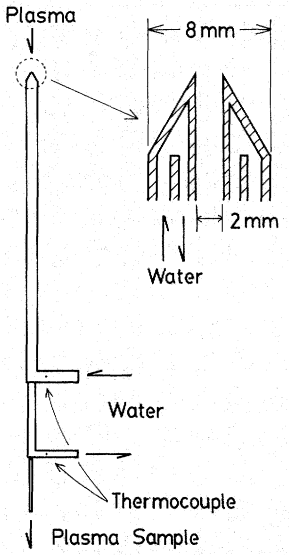

Fig. 7. Schematic of water-cooled probe

coolant channel inlet and outlet.

The plasma gas passed from the probe tip through the central tube and then to a gas chromatograph or to a flow meter. The probe was capable of accurate local measurements because of its small size (2 mm-i.d. and 8 mm-o.d.)

1) Temperature measurements The temperature of the RF plasma was determined by a calorimetric method. The coolant temperature rise and flow rate were measured when a valve in the gas sample line was closed. The same procedure was repeated when the valve was opened, with measurements of the gas flow rate. The plasma enthalpy was given by the difference between the two measurements:

$$(h_1-h_2)\dot{m}_{Ar}=\dot{m}_{H_2O}C_{P_{H_2O}}\Delta T \tag{26}$$

2) Velocity measurements The water-cooled probe was used as a Pitot tube to determine the plasma velocity. The Bernoulli equation provides the following equation:

$$\Delta P=C\frac{1}{2}\rho u^2 \tag{27}$$

The plasma axial velocity was obtained from measured pressure rise ΔP. The coefficient of a Pitot tube, C, was taken to be equal to 1.20.[2]

3) Concentration measurements The concentrations of argon and helium in the RF plasma were obtained by gas chromatography.

2.3 Experimental results

Experimental measurements were made for an argon-helium plasma operated at a power level of 8 kW for argon at 20 litre/min ($Q1=10$ litre/min, $Q2=10$ litre/min) and helium at 5 litre/min ($Q3$).

Calculated and measured results are compared in **Figs. 8** to **10** for the temperature, axial velocity and

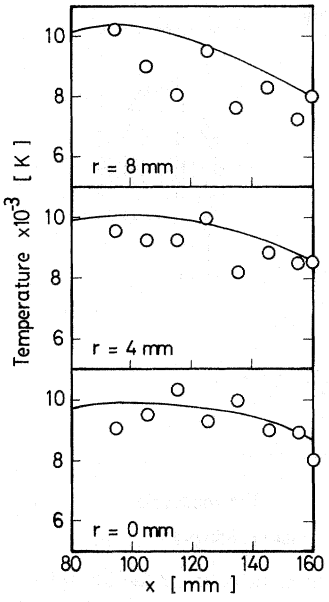

Fig. 8. Comparison of calculated (solid lines) and measured (keys) temperature profiles (Ar: $Q1 = 10$ litre/min, $Q2 = 10$ litre/min; He: $Q3 = 5$ litre/min)

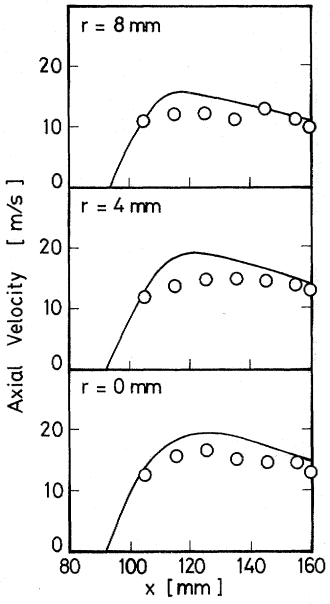

Fig. 9. Comparison of calculated (solid lines) and measured (keys) axial velocity profiles (Ar: $Q1 = 10$ litre/min, $Q2 = 10$ litre/min; He: $Q3 = 5$ litre/min)

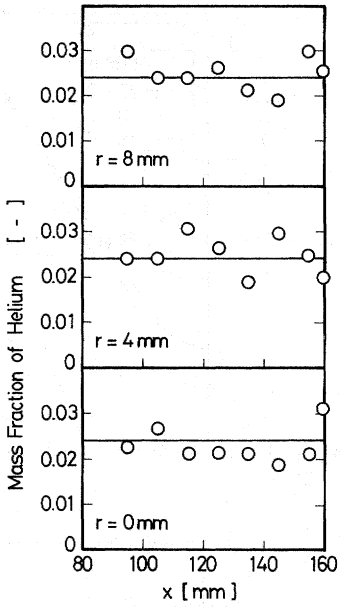

Fig. 10. Comparison of calculated (solid lines) and measured (keys) helium concentration profiles (Ar: $Q1 = 10$ litre/min, $Q2 = 10$ litre/min; He: $Q3 = 5$ litre/min)

helium concentration, respectively. These results show agreement between the calculated and the measured profiles, indicating the validity of this numerical model. The assumption of laminar flow is reasonable since the exit Reynolds number was on the order of 10. A small difference in these figures results from the disturbance in the RF plasma caused by the probe and from the imperfection of the calculation model; the water-cooled nozzle (30 mm-i.d.) at the torch exit was not considered in the calculation model.

Conclusions

A mathematical model for the numerical simulation of an argon-helium mixed thermal RF plasma under atmospheric pressure was formulated. The two-dimensional flow, temperature and concentration fields were obtained with the physical properties of the argon-helium mixture being taken into account.

A water-cooled probe was used to measure the axial velocity, temperature and concentration of the argon-helium plasma. The measured results showed agreement with the calculated ones. The agreement between these results indicated the validity of the numerical model.

The characteristics of an argon-helium RF plasma are as follows:

1) The recirculating eddy formed by the electromagnetic pumping effect becomes stronger in an argon-helium plasma than that in an argon plasma.

2) A uniform distribution of helium is obtained upstream from the discharge region.

Nomenclature

C	=	coefficient of Pitot tube	[—]
C_P	=	specific heat at constant pressure	[J kg^{-1} K^{-1}]
C_w	=	mass fraction	[—]
D_i	=	diffusion coefficient	[m^2 s^{-1}]
E_i	=	ionization energy	[J]
E	=	electric field	[V m^{-2}]
F_r	=	body force	[N m^{-3}]
H_x	=	magnetic field	[A m^{-1}]
h	=	enthalpy	[J kg^{-1}]
h_p	=	Planck's constant	[J s]
I	=	coil current	[A]
k	=	thermal conductivity	[W m^{-1} K^{-1}]
k_b	=	Boltzmann's constant	[J K^{-1}]
k_c	=	thermal conductivity of quartz tube	[W m^{-1} K^{-1}]
L	=	length	[m]
m	=	molecular weight	[kg]
$\dot{m}$	=	mass flow rate	[kg s^{-1}]
N	=	number of coil turns	[—]
n	=	number density	[m^{-3}]
P	=	local power input	[W m^{-3}]
p	=	pressure	[Pa]
ΔP	=	measured pressure rise	[Pa]
Q_r	=	radiation loss per unit volume	[W m^{-3}]
$Q1, Q2$	=	input flow rate of argon	[litre min^{-1}]
$Q3$	=	input flow rate of helium	[litre min^{-1}]
r	=	distance in radial direction	[m]
R	=	inside radius of torch	[m]
R_c	=	coil radius	[m]
T	=	temperature	[K]
ΔT	=	difference of coolant temperature rise between that with valve opened and that with valve closed	[K]
U	=	partition function	[—]
u	=	axial velocity	[m s^{-1}]
v	=	radial velocity	[m s^{-1}]

W	=	thickness of quartz tube	[m]
x	=	distance in axial direction	[m]
μ	=	viscosity	[Pa s]
ξ	=	magnetic permeability of vacuum	[H m^{-1}]
ω	=	oscillator frequency	[rad s^{-1}]
ρ	=	density	[kg m^{-3}]
σ	=	electrical conductivity	[mhos m^{-1}]
χ	=	phase difference between electric and magnetic fields	[rad]

〈Subscript〉

Ar	=	argon
e	=	electron
He	=	helium
H_2O	=	cooling water
i	=	i-th ion of argon
1	=	probe entrance
2	=	probe exit

Literature Cited

1) Boulos, M. I.: *IEEE Trans. Plasma Sci.*, **PS-4**, 28 (1976).
2) Chue, S. H.: *Prog. Aerospace Sci.*, **16**, 147 (1975).
3) Devoto, R. S.: *Phys. Fluids*, **16**, 616 (1973).
4) Devoto, R. S. and C. Li: *J. Plasma Phys.*, **2**, 17 (1968).
5) Evans D. L. and R. S. Tankin, *Phys. Fluids*, **10**, 1137 (1967).
6) Gray, J., P. F. Jacobs and M. P. Sherman: *Rev. Sci. Instruments*, **33**, 738 (1962).
7) Guo-Ying, Z. and Z. Ching-Wen: *IEEE Trans. Plasma Sci.*, **PS-14**, 531 (1986).
8) Hirschfelder, J. O., C. F. Curtiss and R. B. Bird: "Molecular Theory of Gases and Liquids", 539, John Wiley and Sons, New York (1964).
9) Hsu, K. C. and E. Pfender: Proc. ISPC-5, 144 (1985).
10) Mensing, A. E. and L. R. Boedeker: *NASA Contractor Report*, **CR 1312** (1969).
11) Miller, R. C. and R. J. Ayen: *J. Appl. Phys.*, **40**, 5260 (1969).
12) Mostaghimi, J., P. Proulx and M. I. Boulos: *Num. Heat Transfer*, **8**, 187 (1985).
13) Patanker, S. V.: "Numerical Heat Transfer and Fluid Flow", McGraw-Hill, New York (1980).
14) Reid, C. R., J. M. Prausnitz and T. K. Sherwood: "The Properties of Gases and liquids", McGraw-Hill, New York (1977).

(Presented at the 54th Annual Meeting of the Society of Chemical Engineers, Japan, at Kobe, April 1989)